1 **Supporting Information**

2 **Conductive and Sodiophilic Ag Coating Layer Regulating Na Deposition**

3 **Behaviors for Highly Reversible Sodium Metal Battery**

4

5 Xiaomin Chen,[+a] Xunzhu Zhou,[+a,b] Zhuo Yang,[a] Zhiqiang Hao,[a,b] Jian Chen,[a] Wenxi Kuang,[a] Xiaoyan

6 Shi,[a] Xingqiao Wu,[a,b] Lin Li*[a,b], and Shu-Lei Chou*[a,b]

7

8 [a] X. Chen, Dr. X. Zhou, Z. Yang, Dr. Z. Hao, J. Chen, W. Kuang, X. Shi, Prof. X. Wu, Prof. L. Li,

9   Prof. S.-L. Chou

10   Department Institute for Carbon Neutralization, College of Chemistry and Materials Engineering,

11   Wenzhou University

12   Wenzhou, Zhejiang 325035, China

13   E-mail: linli@wzu.edu.cn; chou@wzu.edu.cn

14 [b] Dr. X. Zhou, Dr. Z. Hao, Prof. X. Wu, Prof. L. Li, Prof. S.-L. Chou

15   Wenzhou Key Laboratory of Sodium-Ion Batteries, Wenzhou University Technology Innovation

16   Institute for Carbon Neutralization

17   Wenzhou, Zhejiang 325035, China

18

19 [+] These authors contributed equally: Xiaomin Chen, Xunzhu Zhou

1 **Experimental Procedures**

2 **Materials.** Sodium hexafluorophosphate ($NaPF_6$, battery-grade) and diethylene glycol dimethyl ether

3 (G2, battery-grade) were purchased from Duoduo chemical reagent Co., Ltd. The electrolyte of 1.0 M

4 $NaPF_6$-G2 was mixed inside a glove box with O_2 and H_2O content < 0.1 ppm. Na metal (99.7%, Aladdin)

5 was rolled and pressed as Na chips (10 mm diameter) before assembling batteries.

6 Preparation of Zn@Ag electrode: Ag was deposited on commercial Zn foil by thermal evaporation

7 and magnetron sputtering. 50 nm is the set value on high vacuum resistance evaporation coating machine

8 (ZD-400). The Cu/Zn/Zn@Ag foils were then cut into 10 mm circular pieces.

9 80% commercial Prussian blue (PB), 10% ketjen black (KB) and 10% water-based binder was used

10 to prepare the cathode slurry. And then, the slurry was coated onto an aluminum foil and dried at 80 °C

11 for 12 h in vacuum. In addition, the cathode electrodes were dehydrated at 180 °C for 2 h before

12 assembling the batteries. The active material loading is ca. 1.0 mg cm^{-2} on each electrode. High loading

13 PB cathode for assembling the anode-free batteries is ca. 12.0 mg cm^{-2}.

14 **Electrochemical measurements and cell assembly.** CR2032-type coin cells were assembled in an

15 Ar-filled glovebox. Al_2O_3-Polypropylene (PP) separator is selected as the separator with 60 μL

16 electrolyte. The performance of these cells was tested on a NEWARE battery cycler (CT-3008W). The

17 Tafel plot, electrochemical impedance spectroscopy (EIS), and cyclic voltammetry (CV) were measured

18 on a CHI600C electrochemical workstation (Chenhua).

19 **Tafel plots:** Symmetric Zn-Na||Zn-Na and Zn@Ag-Na||Zn@Ag-Na cells are assembled in Figure 3d,

20 where 1.0 mAh cm^{-2} Na was pre-deposited. The exchange current density was calculated by Tafel curve

21 to evaluate the ion transfer kinetics at the electrode-electrolyte interface. The scan rate is 1.0 mV s^{-1}, the

22 voltage range is from -0.02 V to 0.02 V. The relationship between overpotential (η) and current density

23 (i) in Tafel formula is as follows:[1]

24 $\eta = a + b \times \log|i|$ (Eq. S1)

25 where the constant a is the overpotential when i is equal to the unit current density, and the constant

26 b is termed the Tafel slope.

1   **Electrochemical impedance spectroscopy (EIS):** Symmetric Zn-Na‖Zn-Na and Zn@Ag-

2   Na‖Zn@Ag-Na cells are assembled in Figure 3e, 5a and S6, where 1.0 mAh cm^{-2} Na was pre-deposited.

3   EIS was recorded from 100 kHz to 0.01 Hz. The activation energy is calculated through varying-

4   temperature EIS from 273 to 323 K based on the Arrhenius formula.

5   **Cyclic voltammetry (CV)**: Zn-Na‖PB and Zn@Ag-Na‖PB cells are assembled in Figure 4a, where

6   1.0 mAh cm^{-2} Na was pre-deposited. CV was carried out with the scan rate of 0.1 mV s^{-1} at 1.5-3.7 V.

7   **Other electrochemical performance:** Long-term cycling performance of Zn-Na‖Na and Zn@Ag-

8   Na‖Na cells were assembled in Figure 3a and 3b with the current density of 0.5 mA cm^{-2} for 3 h, where

9   2.0 mAh cm^{-2} Na was pre-deposited. The rate performance of Zn-Na‖Na and Zn@Ag-Na‖Na cells were

10   assembled in Figure 3c with the current density of 1.0 to 5.0 mA cm^{-2} for 1 h, where 6.0 mAh cm^{-2} Na

11   was pre-deposited. The thickness of Na foil is 0.448 mm.

12   Long-term cycling of symmetric Zn-Na‖Zn-Na and Zn@Ag-Na‖Zn@Ag-Na cells were assembled in

13   Figure S5 with the current density of 0.5 mA cm^{-2} for 3 h, where 2.0 mAh cm^{-2} Na was pre-deposited.

14   Nucleation overpotential is tested by the asymmetric Zn‖Na, Zn@Ag‖Na, Cu‖Na or Al‖Na cells in

15   Figure 2a and S1 with the current density of 0.5 mA cm^{-2}. And the same assembly is appropriate for the

16   Coulombic efficiency in Figure 3f and S7-10. The current density is 0.5 mA cm^{-2} in Figure 3f and S7-9

17   and 1.0 mA cm^{-2} in Figure S10.

18   Half Na‖PB cells are assembled in Figure S11 for comparison with the current density of 50 mA g^{-1}.

19   Anode-less Zn-Na‖PB, Zn@Ag-Na‖PB, Cu-Na‖PB, and Al-Na‖PB cells are assembled in Figure 4b-

20   4g, S10 and S12-15, where 1.0 mAh cm^{-2} Na was pre-deposited. The current density is 50 mA g^{-1} or

21   100 mA g^{-1}.

22   Anode-free Zn‖PB, Zn@Ag‖PB, Cu‖PB, and Al‖PB cells are assembled in Figure 5c-5e and S16,

23   with the charge current density of 20 mA g^{-1} and discharge current density of 50 mA g^{-1}.

24   **Characterizations.** The morphology and thickness of deposited Na on Zn and Zn@Ag foils were

25   observed via scanning electron microscopy (SEM 3100, CIQTEK Ltd.). The wettability of electrolyte

26   on Zn foil or Zn@Ag foil was tested by contact angle system (CA100C, INNUO Ltd.).

1   **Theoretical calculations.** Density functional theory (DFT) calculations were carried out using the

2   Gaussian 09 package. Such calculations were performed using Vienna ab-initio simulation package

3   (VASP) with the generalized gradient approximation (GGA) and the Perdew-Burke-Eznerhof (PBE)

4   functional (GGA-PBE) to describe the exchange-correlation energy of electrons.[2] DFT calculations

5   were applied to calculate the adsorption energy between a Na atom and the metal surfaces with largest

6   XRD intensity, namely, Ag (100) and Zn (101).

7

a

b

c   Zn Lα1,2
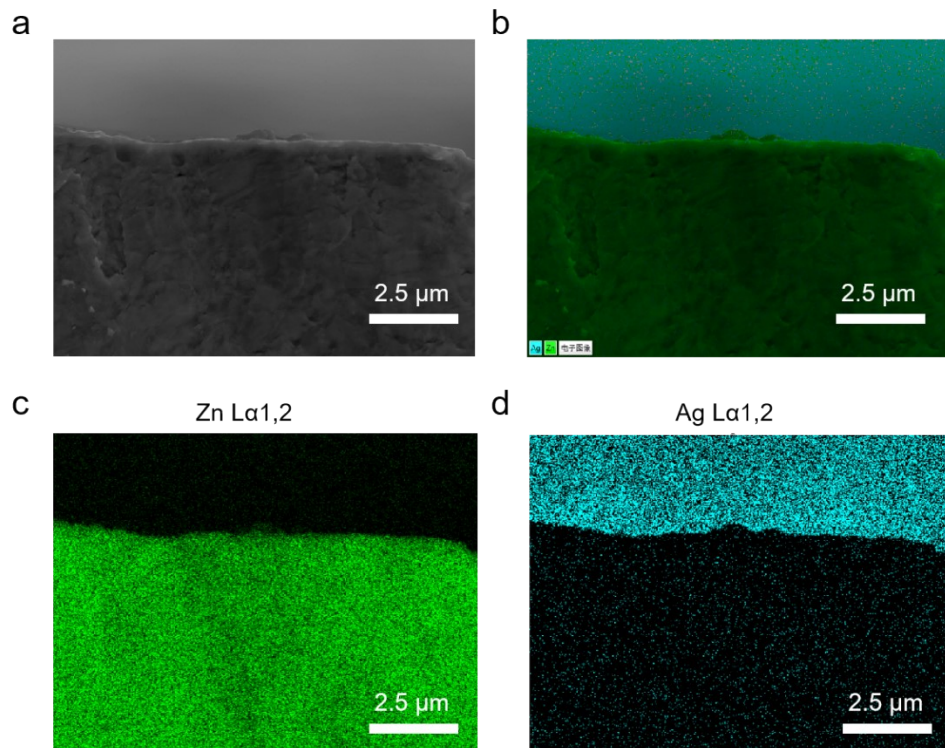
d   Ag Lα1,2

Figure S1. (a) SEM image of Zn@Ag substrate and (b-d) the corresponding elemental mapping images.
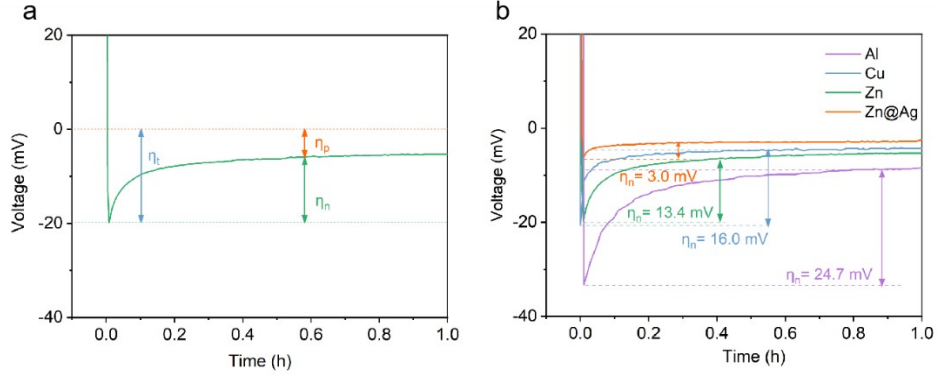
1

2 **Figure S2.** (a) Schematic diagram of tip overpotential (η_t), plateau overpotential (η_p) and nucleation

3 overpotential (η_n), where η_n is defined as the voltage gap between η_t and η_p. (b) Galvanostatic discharge

4 voltage profiles of Na deposition at 0.5 mA cm^{-2} on Al, Cu, Zn and Zn@Ag substrate.

5

6 According to the classical nucleation theory, the Gibbs free energy of the heterogeneous nucleus is

7 calculated as following:[3-5]

8
$$\Delta g_{nuli} = \Delta g_{bulk} + \Delta g_{surf} = -\frac{2\pi r^3}{3}\frac{zF\eta}{V_m} + 2\pi r^2 \gamma_{SL} \qquad (Eq.\,S2)$$

9 where V_m is the molar volume of Zn, γ_{SL} the surface free energy of Zn-electrolyte interface, z the number

10 of electrons per monomer unit, F the Faraday's constant, η the nucleation overpotential. From the

11 equation $d\Delta g_{nuli}/dr = 0$, the critical nucleation radius r_{crit} can be obtained:

12
$$r_{crit} = \frac{2V_m\gamma_{SL}}{zF\eta} \qquad (Eq.\,S3)$$

13 For a semi-spherical nucleus, the critical nucleation volume $V_{crit} = \frac{1}{2}\frac{4\pi}{3}r_{crit}^3$. By inserting V_{crit} one

14 obtains the areal nucleation density N_{crit}:

15
$$N_{crit} = \frac{3z^3F^3\eta^3}{16\pi N_A V_m^2 \gamma_{SL}^3} \qquad (Eq.\,S4)$$

16 where N_A is the Avogadro constant.

1   In a fixed electrolyte, nucleation overpotential η_n play a crucial role on regulating the initial nucleation

2   behavior. That is, the initial nucleus size is inversely proportional to nucleation overpotential, and the

3   nucleation density is proportional to the cube of nucleation overpotential.
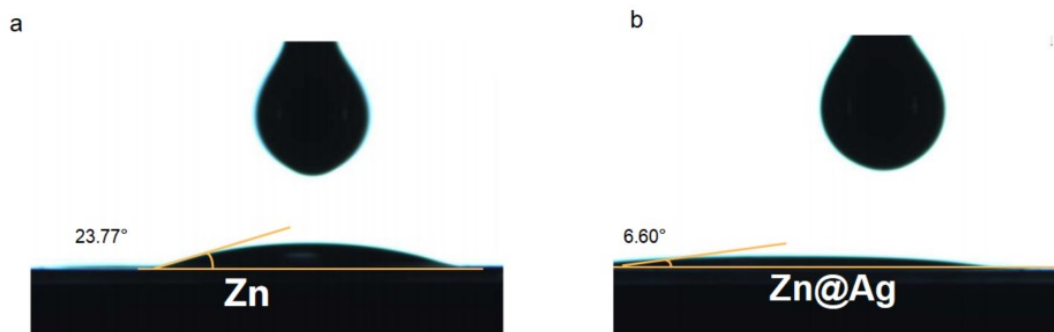
1

2 **Figure S3.** Contact angle of 1.0 M NaPF$_6$-G2 electrolyte on (a) Zn and (b) Zn@Ag substrates.

3
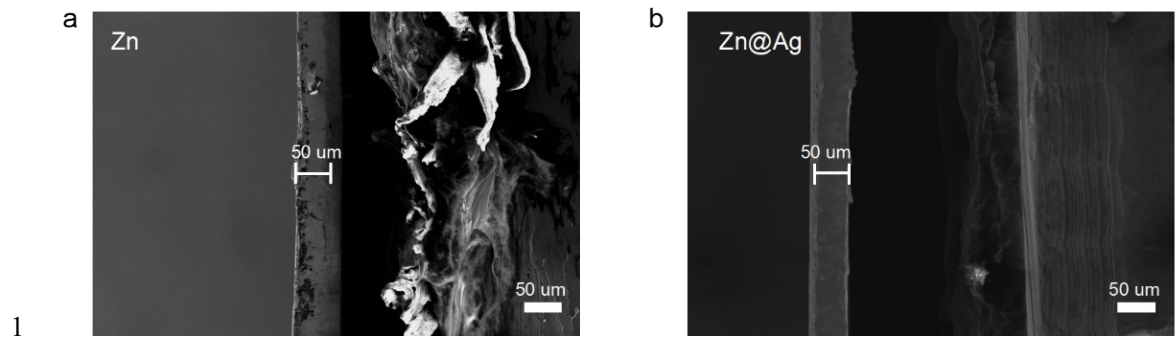
Figure S4. Cross-sectional SEM images of pristine (a) Zn foil and (b) Zn@Ag foil.

1
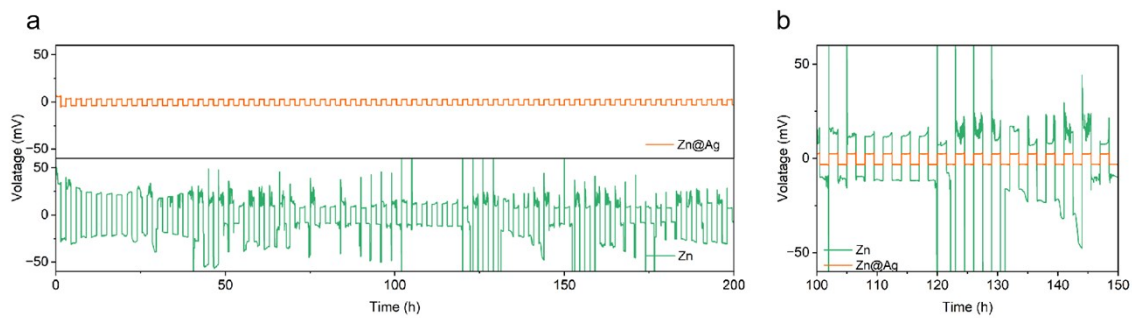
2

3 **Figure S5.** (a) Long-term cycling of Zn-Na‖Zn-Na and Zn@Ag-Na‖Zn@Ag-Na cells and (b) the

4 corresponding enlarged voltage-time profiles with the current density is 0.5 mA cm^{-2} for 3 h. The pre-

5 deposited Na is 2.0 mAh cm^{-2}.

6

1
2
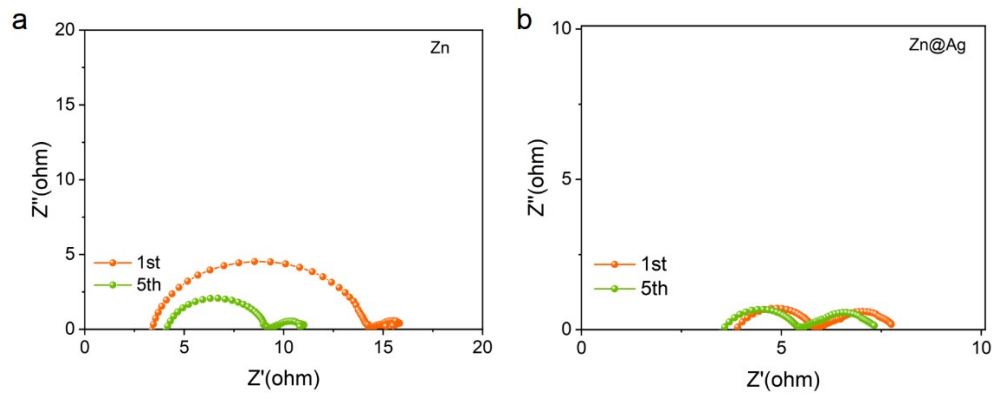
3

4 **Figure S6.** Comparison of EIS of (a) Zn-Na‖Na and (b) Zn@Ag-Na‖Na cells after the first and fifth

5 cycles.

6
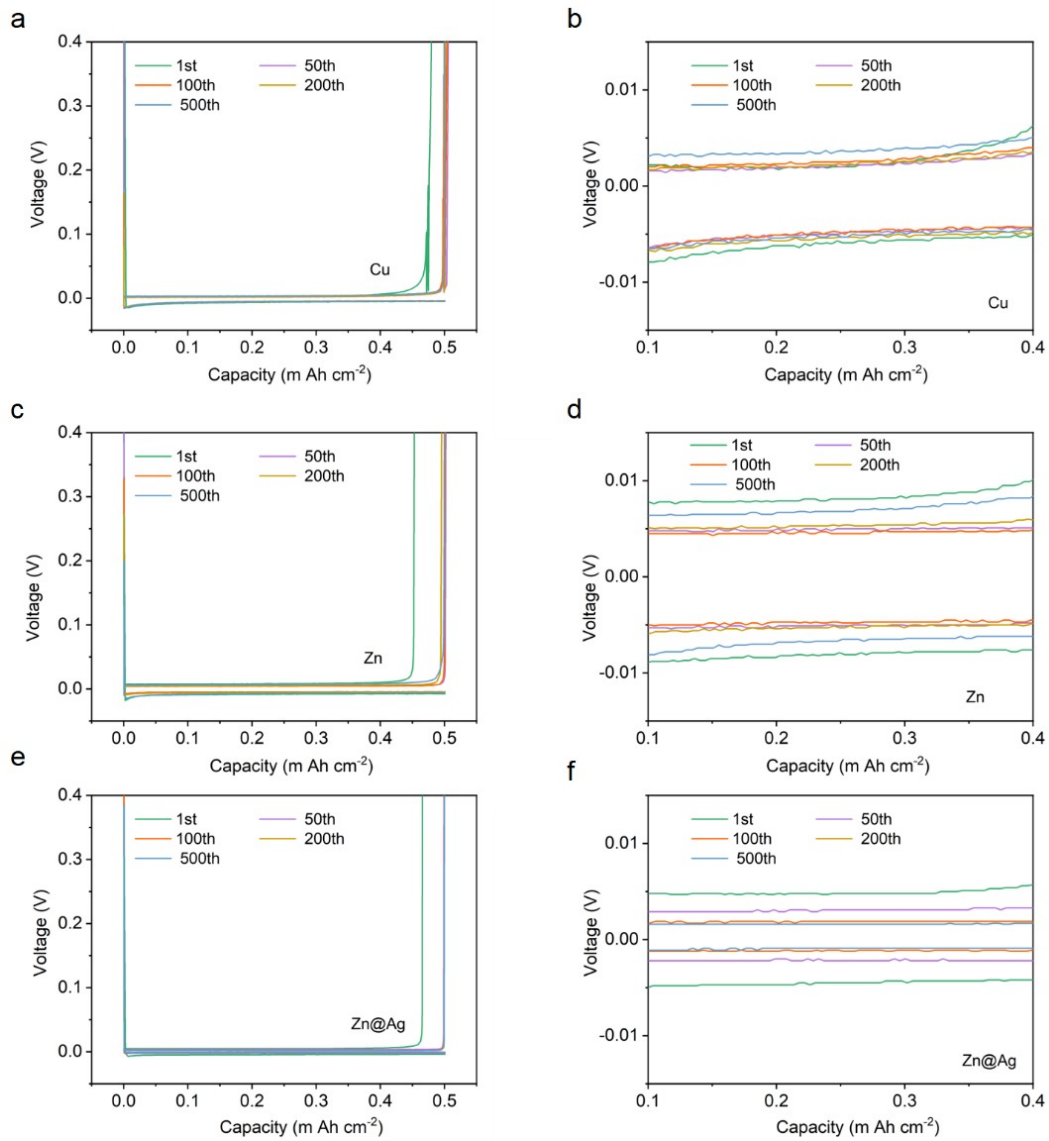
Figure S7. Galvanostatic Na plating/stripping voltage profiles at selected cycles of (a, b) Cu||Na, (c, d) Zn||Na, and (e, f) Zn@Ag||Na cells.

a

b
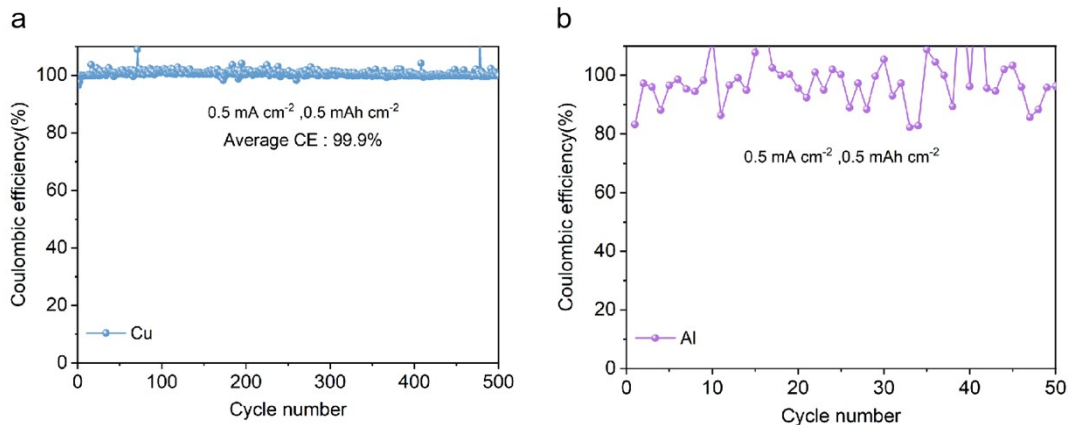
1

2 **Figure S8.** Coulombic efficiency of (a) Cu||Na cell and (b) Al||Na cell at 0.5 mA cm^{-2} for 0.5 mAh
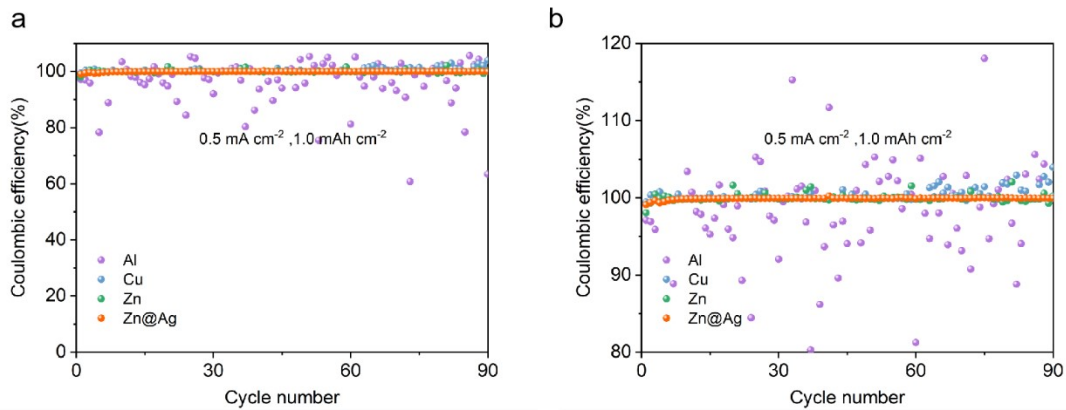
3 cm^{-2}.

Figure S9. (a) Coulombic efficiency of Na on Al, Cu, Zn, and Zn@Ag substrates at 0.5 mA cm^{-2} for 1.0 mAh cm^{-2}. (b) Enlarged curve of (a).
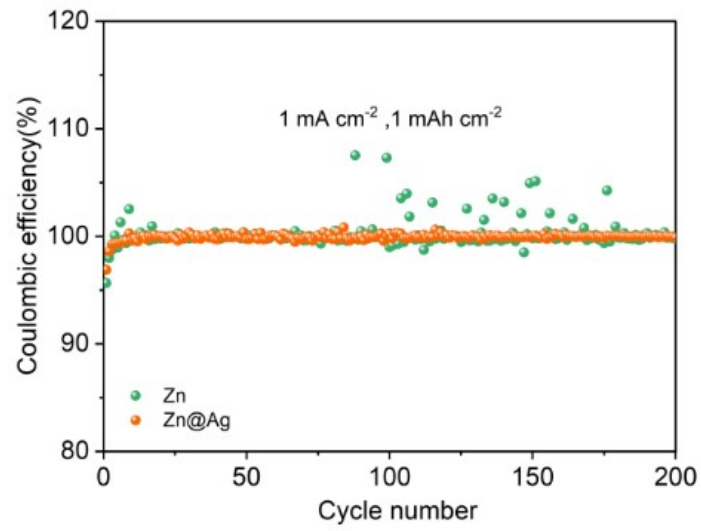
1

2 **Figure S10.** Coulombic efficiency of Zn||Na and Zn@Ag||Na cells at 1.0 mA cm^{-2} for 1.0 mAh cm^{-2}.

3
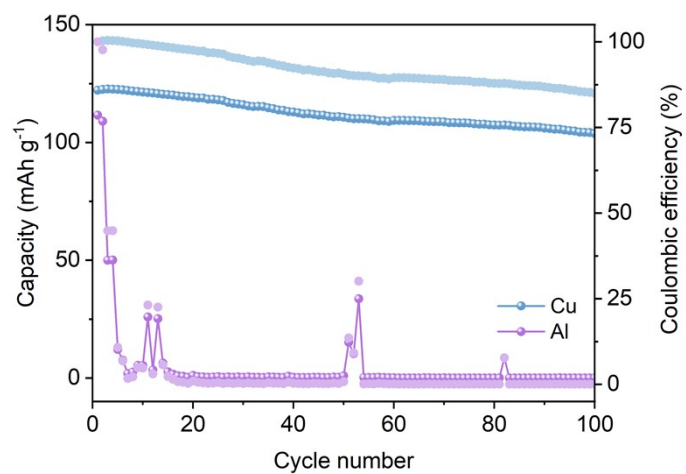
1

2 **Figure S11.** Cycling performance of anode-less Cu-Na‖PB and Al-Na‖PB half-cell at 50 mA g^{-1}.

3
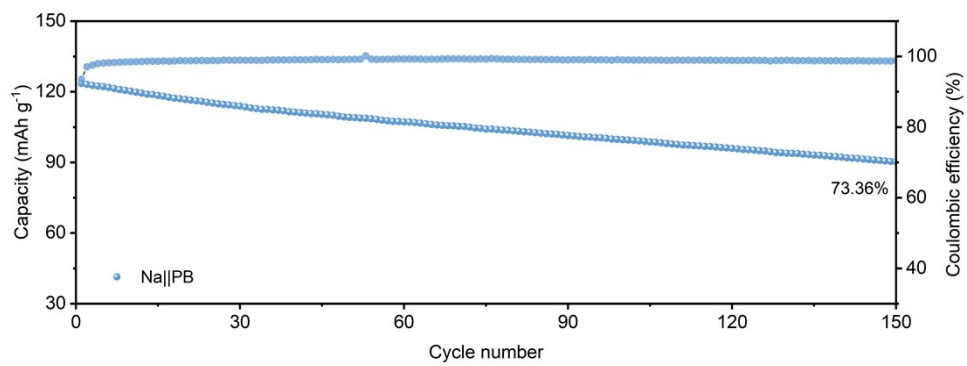
1

2 **Figure S12.** Cycling performance of Na||PB half-cell at 50 mA g^{-1}.

3
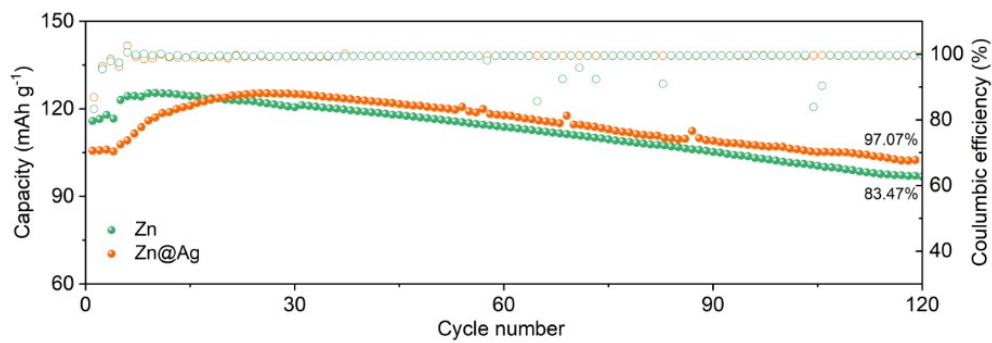
1

2 **Figure S13.** Cycling performance of anode-less Zn-Na||PB and Zn@Ag-Na||PB cells at 100 mA g^{-1}.

3
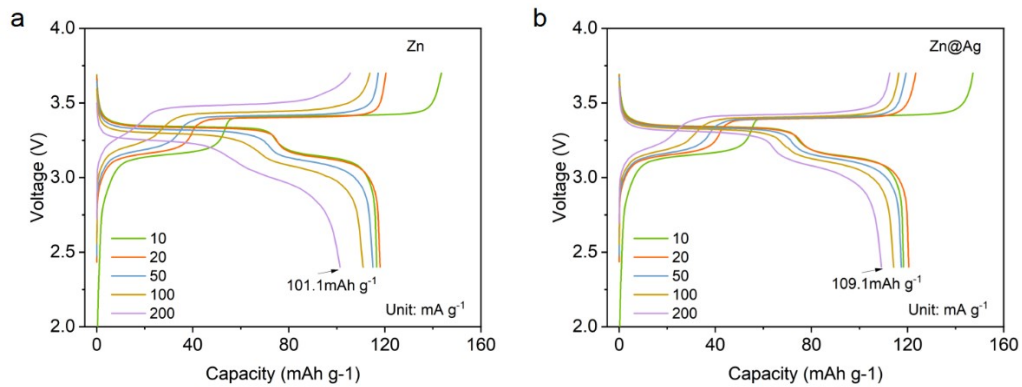
Figure S14. Charge/discharge profiles of anode-less (a) Zn-Na||PB and (b) Zn@Ag-Na||PB cells during the rate performance.
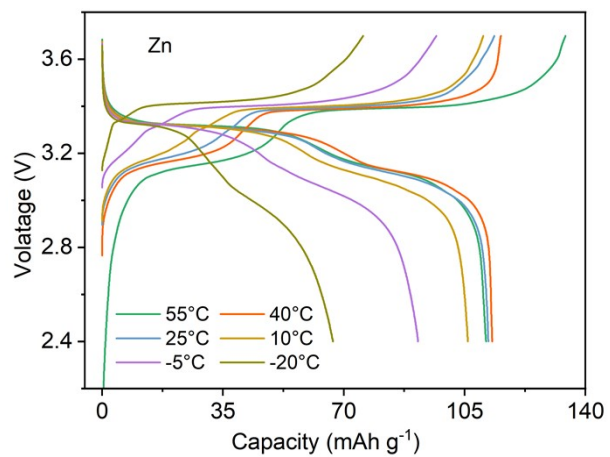
1

2 **Figure S15.** Charge/discharge profiles of anode-less Zn-Na||PB cell from 55 to -20 °C.

3
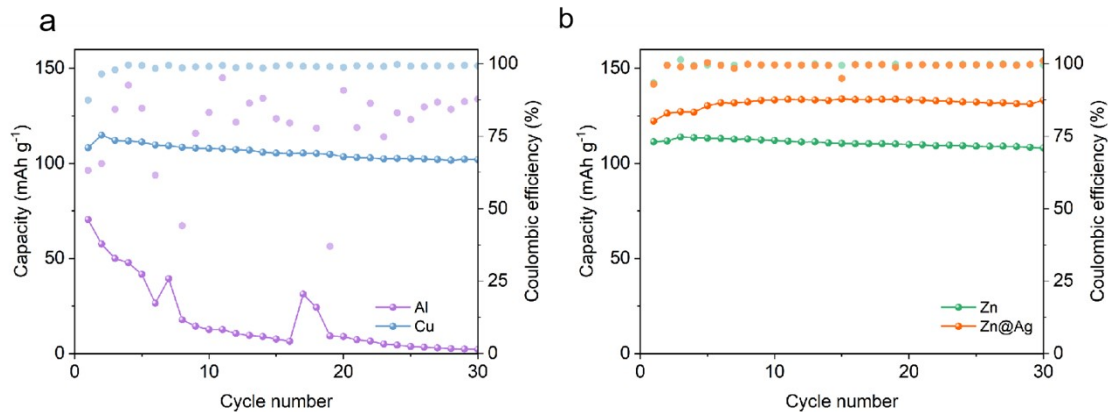
1

2 **Figure S16.** Long-term cycling of anode-less (a) Al-Na||PB, Cu-Na||PB cell and (b) Zn-Na||PB,

3 Zn@Ag-Na||PB cells at -20 °C.

4
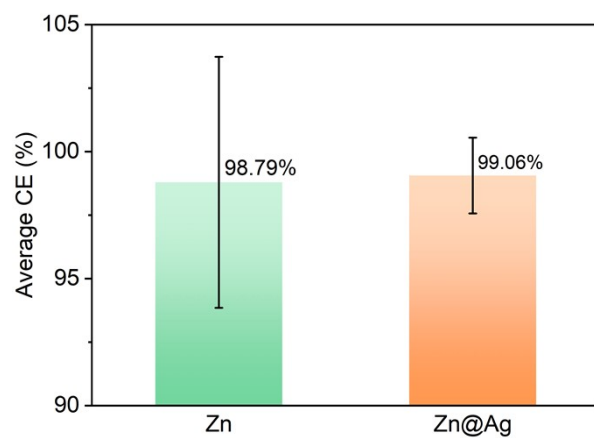
1

2 **Figure S17.** Average Coulombic efficiency of anode-free Zn‖PB and Zn@Ag‖PB cells.

3

Table S1. Radar map of various overpotentials and initial Na loss of Cu‖Na, Al‖Na, Zn‖Na and Zn@Ag‖Na cells.

Substrate	η_t (mV)	η_p (mV)	η_n (mV)	ΔE (mV)	Initial Na loss
Cu	20.7	4.7	16.0	10.0	3.5%
Al	33.3	8.6	24.7	21.2	17.7%
Zn	17.7	7.7	10.0	15.9	9.1%
Zn@Ag	7.3	3.9	3.3	8.0	2.6%

References:

[1] Wan, F.; Zhou, X.; Lu, Y.; Niu, Z.; Chen, J. Energy Storage Chemistry in Aqueous Zinc Metal Batteries. *ACS Energy Lett.* **2020,** *5*, 3569-3590.

[2] Perdew, J. P.; Burke, K.; Ernzerhof, M. Generalized Gradient Approximation Made Simple. *Phys. Rev. Lett.* **1996**, *77*, 3865.

[3] Plieth, W. Electrochemistry for Materials Science; *Elsevier: Amsterdam*, **2008**; pp 195-203.

[4] Pei, A.; Zheng, G.; Shi, F.; Li, Y.; Cui, Y. Nanoscale Nucleation and Growth of Electrodeposited Lithium Metal. *Nano Lett.* **2017**, *17,* 1132-1139.

[5] Zhou, X.; Zhang, Q.; Hao, Z.; Ma, Y.; Drozhzhin, O. A.; Li, F. Unlocking the Allometric Growth and Dissolution of Zn Anodes at Initial Nucleation and an Early Stage with Atomic Force Microscopy. *ACS Appl. Mater. Interfaces* **2021,** *13*, 53227-53234.